

Surface pH controls purple-to-blue transition of bacteriorhodopsin

A theoretical model of purple membrane surface

Istvan Szundi and Walther Stoeckenius

Cardiovascular Research Institute and Department of Biochemistry and Biophysics, University of California, San Francisco, California 94143

ABSTRACT We have developed a surface model of purple membrane and applied it in an analysis of the purple-to-blue color change of bacteriorhodopsin which is induced by acidification or deionization. The model is based on dissociation and double layer theory and the known membrane structure. We calculated surface pH, ion concentrations, charge density, and potential as a function of bulk pH and concentration of mono- and divalent cations. At low salt concentrations, the surface pH is significantly lower than the bulk pH

and it becomes independent of bulk pH in the deionized membrane suspension. Using an experimental acid titration curve for neutral, lipid-depleted membrane, we converted surface pH into absorption values. The calculated bacteriorhodopsin color changes for acidification of purple, and titrations of deionized blue membrane with cations or base agree well with experimental results. No chemical binding is required to reproduce the experimental curves. Surface charge and potential changes in acid, base and cation titrations are

calculated and their relation to the color change is discussed. Consistent with structural data, 10 primary phosphate and two basic surface groups per bacteriorhodopsin are sufficient to obtain good agreement between all calculated and experimental curves. The results provide a theoretical basis for our earlier conclusion that the purple-to-blue transition must be attributed to surface phenomena and not to cation binding at specific sites in the protein.

INTRODUCTION

Bacteriorhodopsin (bR), the light-driven proton pump in purple membrane (pm) reversibly changes its color from purple ($\lambda_{\max} = 568$ nm) to blue ($\lambda_{\max} = 605$ nm) upon acid titration or removal of cations (1–4). The acid and deionized blue forms are spectroscopically indistinguishable, even in their resonance Raman spectra (5), and acid titration releases cations, cation titration releases protons from the membrane (4, 6). Thus, acid titration and deionization apparently produce the same 'blue membrane'.

The first proposed explanation for the acid transition to blue membrane was that the counterion near the Schiff base becomes protonated and the lack of an M-intermediate in the blue membrane photocycle seemed to support this conclusion (3, 7). After the discovery of deionized blue membrane (4), the primary role in the control of bR color was generally attributed to cation binding, and the dissociation state of the Schiff base counterion was directly linked to the occupancy of binding sites by cations (6, 8–13). Because protons are released from the membrane during cation binding in roughly stoichiometric amounts, indicating that acidic groups are involved, carboxyl groups of protein side chains were generally assumed to form the cation-binding sites (8, 9).

We have explained the role of cations differently and

shown experimentally that the transition must involve protein conformational changes which are controlled by proton concentration at the membrane surface; we concluded that cations affect the transition only by changing the surface pH (14, 15). Native pm contains 25% lipids by weight, 80% of which are strong acids (16, 17), which renders the membrane surface very acidic in the absence of salt. Upon removal of the acidic lipids, or their exchange for neutral lipids, cations no longer affect the pK of the transition, and the deionized membrane remains purple, unless the pH is decreased to <2.0.

We now give a quantitative, theoretical description of the surface properties of pm and the effect of cations on color in the native membrane. The double-layer theory of charged surfaces has been proven a powerful tool in membrane research (for review see reference 18) and we combine it with classical dissociation theory to describe the ionization state of membrane surface groups and the ion distribution near the surface. We show that the experimental data published on the purple-to-blue transition of bR can be explained as consequences of its surface properties, and that arguments advanced to support the role of specific binding sites on the protein should be critically revised.

THEORY

Basic principles

The acidic and basic groups exposed on the purple membrane surface in an aqueous medium produce negative and positive charges, which can be described by dissociation/association constants (K_i). The physical interaction between the charged surface and the ions is described by the double-layer theory. The dissociation/association equilibrium determines the charge density on the membrane surface at any given surface ion concentration, whereas the double-layer theory relates the surface charge density to both surface and bulk ion concentrations.

We consider mono- and divalent cations, and four association processes, for the acidic groups: (a) $A^- + H^+ \rightleftharpoons HA$, dissociation of acid (HA); (b) $A^- + M^+ \rightleftharpoons MA$, binding of a monovalent cation (M^+) to a negative ion (A^-); (c) $A^- + M^{2+} \rightleftharpoons MA^+$, binding of a divalent cation (M^{2+}) to a negative ion; (d) $A_2^{2-} + M^{2+} \rightleftharpoons MA_2$, binding of a divalent cation to two neighboring negative groups, e.g., the two phosphates of the same lipid molecule.

If there are n groups per bR, the balance equation for this acid is $n\text{bR} = A^- + HA + MA + MA^+ + 2MA_2$, where the symbols denote the concentrations of the particular forms.

The number of negative charges per bR (I^-) can be expressed through surface concentrations of the ions and the four association constants:

$$I^- = \frac{A^-}{\text{bR}} = \frac{n}{1 + K_1H^+ + K_2M^+ + K_3M^{2+} + K_4M^{2+}}, \quad (1)$$

where subscript s indicates surface concentrations.¹

Positive charges on the membrane are produced by binding of divalent cations to single negative charges as mentioned above and also by protonation of basic groups (B): (e) $B + H^+ \rightleftharpoons BH^+$.

A third process giving rise to positive surface charges may be the physical absorption/adsorption of hydrophobic cations (OM^+) in/on the membrane which can be formally described by an association process: (f) $OM^+ + \text{bR} \rightleftharpoons \text{bROM}^+$.

The number of positive charges per bR can be calcu-

lated in the following way:

$$I^+ = \frac{MA^+ + BH^+ + \text{bROM}^+}{\text{bR}} \\ = \frac{nK_3M^{2+}}{1 + K_1H^+ + K_2M^+ + K_3M^{2+} + K_4M^{2+}} + \frac{nK_5H^+}{1 + K_5H^+} + K_6OM^+ \quad (2)$$

The numerical value of K_6 can be estimated from the partition coefficient (P) of the hydrophobic cation: $K_6 = P \cdot V_m$, where V_m is the molar volume of bR (≈ 30 liters/mol).

The total charge on the membrane surface (I_t) is the algebraic sum of the positive and negative charges, including all types of acids and bases contained in the membrane

$$I_t = \sum_i I_i^+ - \sum_j I_j^-. \quad (3)$$

The number of charges per bR can be converted into surface charge density (q):

$$q = I_t \times \frac{e}{S}, \quad (4)$$

where e is the absolute value of the electron charge and S is the area occupied by one bR in the membrane.

The surface concentrations (C_s) in Eqs. 1 and 2 can be replaced by bulk ion concentrations (C_b) using the Boltzmann distribution formula:

$$C_s = C_b \exp \left[-\frac{zF\Psi_0}{RT} \right], \quad (5)$$

where z = ion valency, F = Faraday constant, Ψ_0 = surface potential, R = universal gas constant, and T = absolute temperature. In the final form, Eq. 4 contains the known bulk ion concentrations and q and Ψ_0 as unknowns.

For the description of the ion distribution in the electrolyte adjacent to the membrane surface, we substituted the real membrane with an ideally flat surface, where the surface groups are uniformly distributed and localized in the plane of the surface. This is a prerequisite to using the classical electrical double layer theory of ion distribution near a charged surface, which presumes an infinitely large flat surface with uniform distribution of smeared charges. This approximation has been shown to be valid for a variety of charged lipid membranes (19), and because the effects we are going to discuss are caused mainly by membrane lipids, the composition and known geometry of pm allow us to use the same kind of approximation, keeping in mind the limitations imposed on the

¹In Eqs. 1 and 2, it is assumed that $A_2^{2-} = A^-/2$, which does not hold for multiple, competitive interactions. However, it may be a reasonable approximation if only one type of cation binding is considered at a time, and we will discuss only such cases. The general formula is much more complex and will not give us more information on the influence of cations.

system. The Grahame equation relates the surface charge density to surface potential and bulk ion concentrations:

$$q^2 = \frac{RTE}{2\pi} \sum_i C_{ib} \left[\exp \left(\frac{-Z_i F \Psi_0}{RT} \right) - 1 \right], \quad (6)$$

where E is the permittivity of water. Eq. 6 contains the same unknowns (q, Ψ_0) as Eq. 4 in its final form; therefore, when these two equations are combined, q and Ψ_0 can be determined.

The surface concentrations can be obtained by the Boltzmann formula. To calculate ion concentrations at a distance (x) from the surface, we have to replace Ψ_0 with the potential function, $\Psi(x)$. It is, however, not known explicitly in the general case; therefore, we used a step-by-step method (20) to calculate this function. Starting from the potential at zero distance, i.e., the surface potential, Ψ_0 , determined by surface and bulk pH, we first calculated the potential gradient by the known formula (7), then increased the distance from the surface by $\Delta x = 1 \text{ \AA}$ and calculated the new potential as follows:

$$\frac{\delta \Psi}{\delta x} = \left| \frac{8\pi RT}{E} \sum_i C_{ib} \left[\exp \left(-\frac{Z_i F \Psi(x)}{RT} \right) - 1 \right] \right|^{1/2} \quad (7)$$

$$\Psi(x + \Delta x) = \Psi(x) \pm \frac{\delta \Psi}{\delta x} \Delta x. \quad (8)$$

This sequence of computations was continued until $\Psi(x) < 1 \text{ mV}$. The surplus of ions in the double layer (m) is determined by the integral of the excess ion distribution, $c(x) - C_b$, over distance from the membrane surface:

$$m = \int_0^\infty (c(x) - C_b) dx, \quad (9)$$

where $c(x)$ is given by the Boltzmann formula:

$$c(x) = C_b \exp \left(-\frac{ZF\Psi(x)}{RT} \right). \quad (10)$$

To test the accuracy of potential calculation, we determined the surplus of cations and anions in the double layer and compared the algebraic sum of the excess charges with the surface charge density on the membrane. The difference never exceeded 5%, which shows that the numerical method is reasonably accurate.

Although, in most cases, it is the bulk ion concentration that is given in the experiment, in calculations it is often more convenient to use the surface concentration as the known parameter and the bulk value as the unknown. We will always use the surface pH as the known parameter and will consider the bulk concentrations of protons and some other ions as unknown. Because it is very difficult, and sometimes impossible, to give analytical solution of

Eqs. 4 and 6, we have used numerical methods and a computer to solve these equations.

Membrane structure and composition

If the distribution of components over the external and internal surfaces of the membrane were known, the calculations could be done for the two surfaces separately. Although there are indications of an asymmetric lipid distribution across the membrane (21, 22), and the protein structure is known in more detail than for most membrane proteins, too many uncertainties remain and we will use an average membrane composition and not consider the two surfaces separately. We will show later that this is a reasonable approximation.

Purple membrane contains an average of 10 phosphate groups per bR, mainly from (the diether analogue of) phosphatidylglycerophosphate, and approximately two glycolipid sulfate groups (17). In the plane of the membrane, the protein molecules are separated by a single layer of these acidic lipids (23, 24) (Fig. 1 A). The pK of the first dissociation of glycerophosphate is 1.4 and for the second dissociation of the five terminal phosphates, we use pK = 7. Bacteriorhodopsin has 19 aspartic and glutamic acid residues, 14 basic lysine and arginine groups; most of them are presumably near the membrane surface and at least some of them must be ionized. Fig. 1 B shows the most likely distribution of these groups in the membrane according to reference 25. In the calculations, we assume 12 surface carboxyls per bR with pK = 4.7. As will be shown, the results of the calculations are not very sensitive to the number and pK of carboxyl and secondary phosphate groups. The water-exposed basic groups and the sulfolipids should be ionized in the pH range considered in the calculations. Because only the net surface charge is important, we will always indicate only those positive charges, as number of bases per bR, which are in excess and are not involved in the compensation of negative sulfolipids. The actual number of exposed ionized bases in the membrane may be higher by one or two; however, it can not be too high because pm has a net negative charge above pH 2 (26).

RESULTS

Relation between bulk pH and surface pH in the presence of salt

Experimental titrations of bR at constant salt concentrations showed that a 10-fold change in cation concentration shifted the pK of the color transition by 1.0 U for

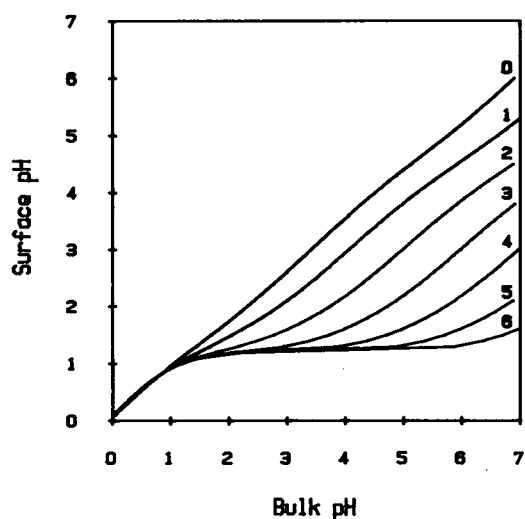


FIGURE 2 Surface pH of pm at 10^0 – 10^{-6} M monovalent electrolyte concentrations. Membrane composition: 10 glycerophosphates (GP), 12 carboxyls (C), 2 bases (B) per bR.

bulk pH at low salt concentrations. In the deionized state, the surface pH of the membrane is very low (≈ 1.0) and it is practically independent of the bulk value. We will call this range the deionized limit.

The low surface pH is not unexpected, because in the absence of other cations, protons must compensate the negative charges of the ionized surface acids. The surface pH is determined by the pK and concentration of lipid glycerophosphates, as we have pointed out before (14, 15). Note that water-exposed carboxyl groups hardly influence the surface pH; only a small shoulder appears

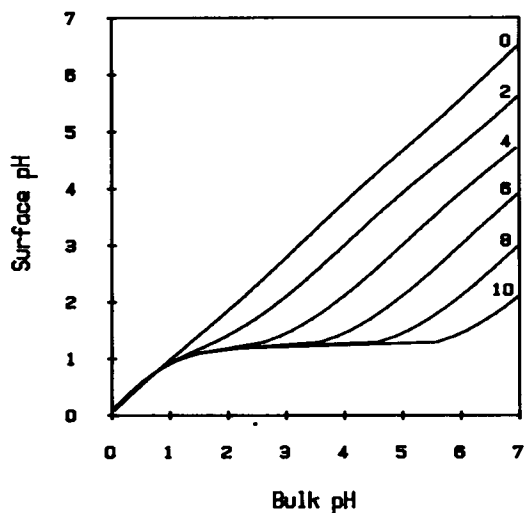


FIGURE 3 Surface pH of pm at 10^0 – 10^{-10} M divalent electrolyte concentrations. Membrane composition as in Fig. 2.

when the surface pH approaches the pK of carboxyl groups. The effect of secondary phosphate dissociation is even less significant (data not shown).

We have also calculated the effects of cation chemical binding and variations in membrane composition on the surface pH curves at 10^{-6} M divalent cation concentration. Introducing cation chemical binding with binding constants 10 M^{-1} for phosphate and 50 M^{-1} for carboxyl, the difference between surface and bulk pH somewhat decreases above the deionized limit, the limit itself, and the curve below it, however, remain the same. The experimentally determined MA^+ association constants for divalent cations and phosphatidylglycerol vesicles are between 5 and 10 M^{-1} (27), which can shift the pH curves by $\approx 0.5 \text{ U}$ roughly parallel to the y axis; MA_2 binding is less effective.

The influence of water-exposed basic groups on the pH curves is fundamentally different from the effect of cation binding (Fig. 4). These positive charges, which are present throughout the weakly alkaline and acidic pH range, reduce the net surface charge and, at low pH, can reverse it. Basic groups will therefore raise the surface pH over the whole bulk pH range. Introducing two, four, and six positive charges per bR increases the deionized limit by a total of $\approx 1.0 \text{ U}$ in $\approx 0.3\text{-U}$ steps. It is unlikely that six positive charges per bR are present on the membrane surface; two basic amino acids are probably deeply buried and some of the amino groups in the protein surface region may be buried too, or involved in internal salt bridges contributing to the stability of protein structure; two may compensate negative sulfolipid charges. It is

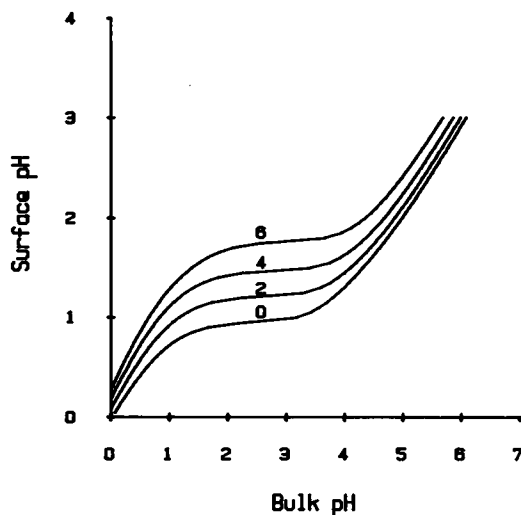


FIGURE 4 Dependence of surface pH on the number of basic groups per bR. Divalent cation: 10^{-6} M . Membrane composition: 10 GP, 12 C, B as indicated on the curves.

more realistic to assume a maximum of two or three net positive charges per bR.

The situation, however, will be quite different if the protein structure is disturbed by physical or chemical means. Exposure of basic amino acid residues to water will increase the number of positive groups without increasing the number of ionized acidic groups if the salt concentration is low, because the carboxyl groups on the surface cannot dissociate at low surface pH. Thus, changing the protein structure will change the charge distribution on the membrane surface, and consequently, the structure of the double layer will change. These changes are directly related to cation-binding phenomena and will be discussed elsewhere.

Reduction of the number of acidic phospholipids also increases the deionized limit of surface pH in a similar manner, except below pH 1, where all the curves merge as expected for neutral surface. With no basic groups present and four glycerophosphate groups per bR, the surface pH is ≈ 1.3 . Two phosphate groups per bR, one on each side of the membrane, still produce a surface pH as low as 1.6. In the presence of two ionized basic groups per bR, reduction of the number of acidic phospholipids has a more pronounced effect on the surface pH (Fig. 5). However, the surface pH is still only ≈ 1.6 if the number of phosphate groups is reduced by 50% to five per bR. A 70% reduction of their number is required to raise the surface pH > 2 .

These data show that the surface pH must be very low on both sides of the membrane, even if the lipid composition is asymmetric. Very large asymmetry in lipid composition or in the number of water-exposed basic groups is

needed to change this situation. The lipid composition (see above) and structural data (24) make this assumption highly unlikely.

Color changes during titrations

The surface pH curves discussed above can be converted into absorption changes of bR. For this purpose the pH dependence of bR absorption has to be measured for a neutral or nearly neutral membrane, because in this case, the surface and bulk pH are the same. We have recently presented acid titration curves for bR color changes in lipid-depleted membrane, and also for bR in a neutral lipid environment (14, 15) and shown that, in these preparations, the pK of the transition is salt-independent and has the same value (1.5–1.9) as in native membrane when the surface charges are screened by high salt concentration (4) or by polycationic polymer adsorption (28). To convert surface pH into absorption values, we have therefore used the average of our HNO_3 and H_2SO_4 titration curves for lipid-depleted membrane.

Fig. 6 shows the calculated absorption maximum (λ_{max}) as a function of bulk pH for monovalent cations in the 10^{-6} – 1.0 M concentration range. Though we used the simplest theoretical description and made several assumptions about the membrane, the qualitative picture agrees well with experiments, and even the quantitative agreement is good (see reference 4). As expected from Figs. 2 and 3, a 10-fold increase shifts the pK of the transition by 1.0 for mono- and 0.5 U for divalent cations.

Whereas the titration curves for native membranes are well described by assuming only acidic groups on the

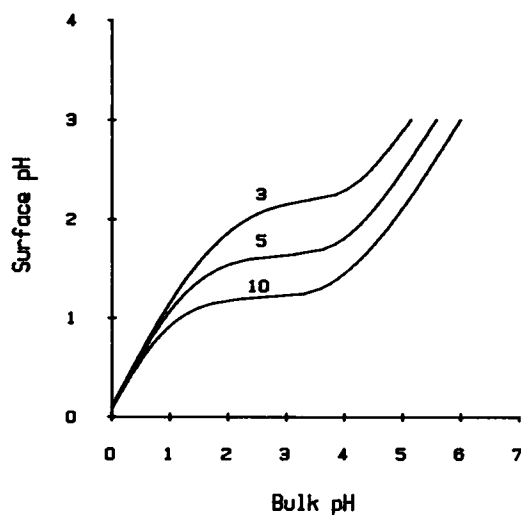


FIGURE 5 Dependence of surface pH on the number of glycerophosphate groups per bR. Divalent cation: 10^{-6} . Membrane composition: GP as indicated, 12 C, 2 B.

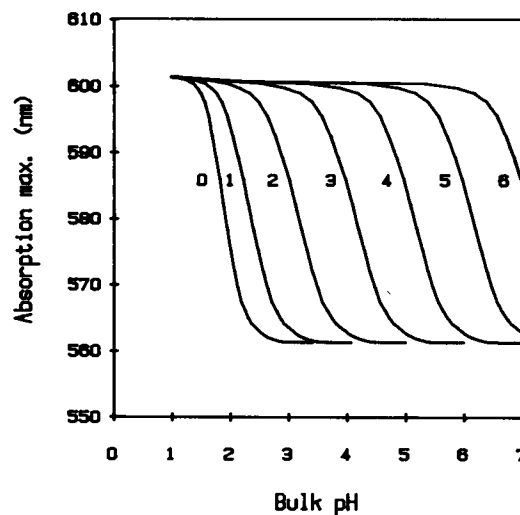


FIGURE 6 Acid titration of bR at 10^0 – 10^{-6} M monovalent electrolyte concentration. Membrane composition as in Fig. 2

membrane surface, it is necessary to include basic groups in the model to reproduce the experimental titration curves of the lipid-depleted membrane. In the absence of basic groups, reduction of the phospholipid content to 30% only slightly raises the deionized limit of surface pH and the acid titration curve for this membrane composition would not be salt-independent. However, by introducing two bases per bR, the titration curve of a membrane with 30% lipid content becomes insensitive to salt concentration (Fig. 7), whereas the titration curve of the membrane with 10 phosphate groups changes very little. Thus, our calculations for 10 phosphate and two basic groups per bR adequately describe the observed color changes of bR in acid titrations. The sometimes-used titration with salt at fixed bulk pH provides no additional information on the system and will be discussed later.

Titration of blue membrane with cations

The number of cations per bR required to induce the same color change is much higher for monovalent than for divalent or trivalent cations (4, 6), which, in our model, is a direct consequence of the double-layer theory, because cations with higher valency displace more protons from the surface layer. Hydrophobic cations are also more effective in inducing the color change (1) and (Helgersen, S. L., M. K. Mathew, and W. Stoeckenius, unpublished results), which is explained by their increased binding due to hydrophobic forces. We will only discuss the interpretation of titration curves for simple divalent cations here because their sigmoidal shape has led to the suggestions

that different binding sites with different effects on the chromophore exist (9) and that cations may act in a cooperative manner (29).

For the cation titration curve of blue membrane, we have to calculate, at every surface pH value, the corresponding number of cations per bR, which comprises the ions in the bulk phase, the chemically bound cations and the ions in the double layer. In these calculations it is assumed that the bulk concentrations of other ions remain unchanged during experimental titration, requiring in practice a bR concentration of $<10^{-6}$ M. In most situations, however, binding of cations to the membrane or in the double layer will change the bulk phase concentration and in cation titrations, the bulk pH decreases because protons are displaced from the surface to the bulk. Therefore, we have to compute the amount of displaced protons and correct the bulk pH accordingly.

The calculated cation titration curves are in good agreement with experimental data (4, 9). The solid curve (Fig. 8a) shows physical, double-layer binding only. Introducing either type of chemical binding, MA^+ or MA_2 with binding constants 10 for phosphate and 50 for carboxyl groups for MA^+ , makes little difference (dashed lines *b* and *c*). A number of cation-binding experiments at constant bulk pH have been reported (12, 13, 30), where blue membrane suspensions were titrated to and maintained at pH 5 with NaOH. Curve *d* in Fig. 8 was calculated to simulate this type of experiment and shows that, in good agreement with the experimental data (30),

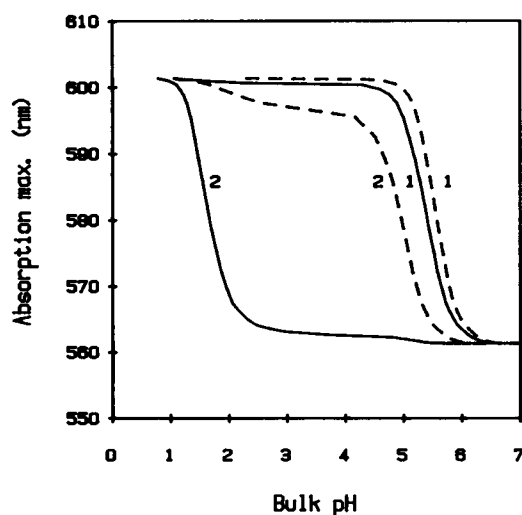


FIGURE 7 Effect of delipidation on the acid titration curve. Divalent cation: 10^{-6} M. Membrane composition: (—) 1: 10 GP, 12 C, 2 B; 2: 3 GP, 12 C, 2 B; (---) 1: 10 GP, 12 C; 2: 3 GP, 12 C.

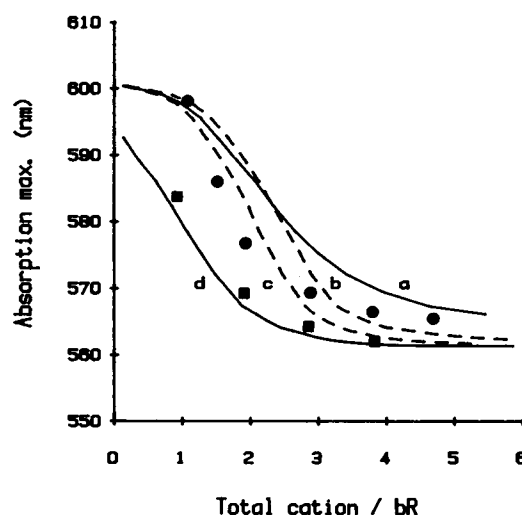


FIGURE 8 Titration of blue membrane with divalent cation. (—) No chemical binding; (---) $K(P) = 10$, $K(C) = 50$ (MA^+). Blue membrane: bR = 10^{-5} M, pH 5. Composition as in Fig. 2. (a-c) Blue membrane pH established with distilled water; (d) blue membrane pH adjusted with NaOH from 4.5 to 5; (b) MA_2 , (c) MA^+ type of binding. Experimental points: (●) reference 4; (■) reference 12.

the sigmoidal shape is lost, and the first added divalent cation already causes a color change, which, in our model, is due to the Na^+ ions in the double layer. When the bulk pH is not controlled by NaOH addition, the influence of the released protons on the cation reconstitution curve is very pronounced at high bR concentrations: at 3×10^{-4} M, the purple color is not regenerated, even at 5–10 added divalent cations per bR.

Our model explains the sigmoidal shape of the titration curve in a simple way. It is unnecessary to assume specific binding sites which affect the chromophore differently. The first cation added and bound in the double layer or on the membrane surface does not induce a color change simply because the surface pH is still too low. More cations are required to change the color. Also, no chemical binding is needed to produce such a titration curve, the binding constants deduced from such experiments have no obvious physical meaning, and the sigmoidal shape of the curve does not necessarily mean that the transition is induced by a cooperative action of cations. The link between the amount of added cation and chromophore absorption is not direct if the color is determined by surface pH. Whether or not the transition itself is a cooperative process is a separate problem.

For most of the calculated curves discussed in this paper, no chemical binding is assumed and they still adequately describe the experimental results. It is known, however, that divalent cations are not removed by extensive washing of purple membrane with distilled water unless exposure to high NaCl concentration preceded the first washing step (6). How can the membrane retain the divalent cations without chemical interaction?

We calculated the number of bound cations and bR absorption shift (i.e., surface pH) as a function of bulk cation concentration for the di- and monovalent cations at 10^{-5} M bR concentration (Fig. 9). No chemical binding was introduced and the released protons were not considered, because they are washed away with distilled water of pH 5.5. Following the dotted line *a* in Fig. 9, we see that most of the monovalent cations bound in the double layer are readily released into the bulk upon dilution and carried away in a few washing steps. Release of 1 cation/bR produces only 10^{-5} M cation in the bulk, which corresponds to only 2 cations/bR in the double layer. The color of the membrane at this stage is almost completely blue ($\lambda_{\text{max}} = 595$ nm). Further reduction of the cation content in the double layer becomes more difficult and it needs ever increasing numbers of washes as the bulk cation concentration is too low to carry away many cations. Following the same reasoning, it is easy to see that divalent cations are difficult to wash away below 4 cations/bR, which corresponds to 10^{-5} M bulk cation concentration and a membrane still purple in color (dotted line *b*). At 3 cations/bR in the double layer, the bulk

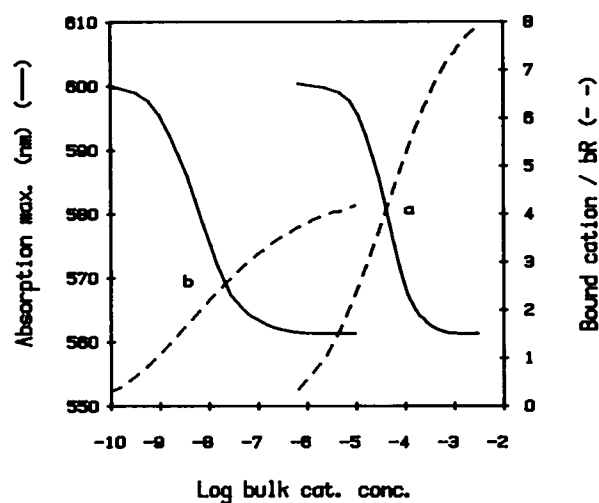


FIGURE 9 bR color and number of double-layer bound cations at different bulk concentrations of (a) monovalent and (b) divalent cations. bR concentration 10^{-5} M, pH 5.5, composition as in Fig. 2.

concentration is as low as 10^{-7} M, which can carry away only 0.01 cation/bR in one washing step. Our model therefore predicts 3–4 divalent cations/bR in well washed pm suspensions, which is in good agreement with experiments (4, 6). Thus it is not necessary to assume chemical binding to explain both the divalent cation content of pm and the need for chelators and ion exchangers to produce blue membrane without significant acidification of the bulk medium.

Titration of blue membrane with base

It has recently been reported that deionized blue membrane could be converted into “deionized purple membrane” by NaOH titration with an apparent pK of 5.4, and the authors argued that the purple membrane at pH >6.0 was still effectively deionized because the amount of Na^+ required to induce the color change in NaOH titration was an order of magnitude less than the NaCl required for titration of a blue membrane at the same initial pH (31, 32). The same argument was also used by other authors to separate pH and Na^+ effects (33). We will show here that the cation and pH effects cannot be treated separately because they are based on a proton-cation competition.

When NaOH is added to a blue membrane suspension, Na^+ will partially replace H^+ in the double layer; the remainder will increase the pH in the bulk phase. At lower bulk $[\text{H}^+]$, proportionally more Na^+ will accumulate in the surface layer and thus a lower bulk $[\text{Na}^+]$ will be required to raise the surface pH above the pK of the transition. The calculated NaOH titration curves (Fig.

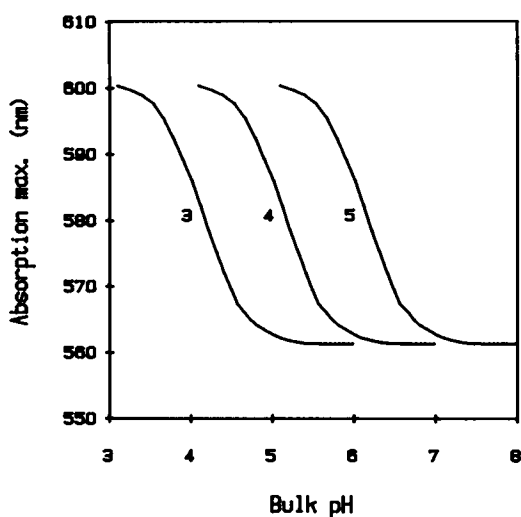


FIGURE 10 Titration of blue membrane with base. bR concentration 10^{-5} M, initial pH as indicated, composition as in Fig. 2.

10) show that the apparent pK of the color change depends on the initial pH of blue membrane suspension. Typically, at 10^{-5} M bR its pH is near 4, and, therefore, the transition will occur between pH 5 and 6 as observed. The total amount of Na^+ per bR required for the transition (Fig. 11) is indeed much less than in NaCl titration, but the reason for the color change in NaOH titration is exactly the same cation effect as in NaCl titration. Blue membranes, at pH 6, can be prepared from deionized blue membrane by thorough washing with deionized water (4) and even above pH 6, when CO_2 is excluded. The model predicts that "deionized purple membrane" containing the native lipids cannot exist. In our model, the color

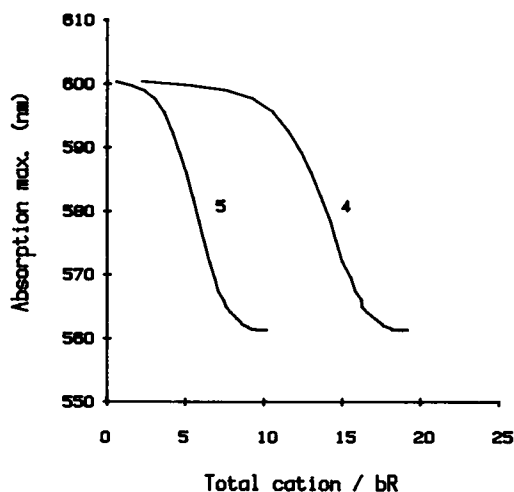


FIGURE 11 bR color as a function of added monovalent cations in base titration. Conditions as in Fig. 10.

change is not a result of true acid-base titration of a carboxyl group with apparent pK of 5.4. The intrinsic pK of the transition used in the calculations is ≈ 1.7 and it is assumed to be independent of cations. Because the model describes the experimental data in every respect, we conclude that the apparent pK found in NaOH titration need not be a bR characteristic. It is merely one of many pK values that can be produced by experimental conditions and can be fully explained by the effect of cations on the difference between surface and bulk pH.

Relation of surface potential and surface charges to color change

Several authors have considered the possibility that electric field changes control the color transition either directly through cation binding to charged groups in the vicinity of the chromophore or through their effect on the macroscopic electric potential of the surface charges (8, 29–31). In our view, the transition is caused only by the surface proton concentration, and its intrinsic pK in pm is below 2 (14, 15). Our calculations contain both surface charge density and potential and we can thus compare the predictions of our model with recent experimental data (31) and also with the electric field effects postulated by others. Fig. 12 shows the surface potential and the number of net negative charges per bR calculated for a titration of blue membrane with divalent cations at constant bulk pH (readjustment with NaOH). Because the surface potential is determined by the difference between bulk and surface pH, $\Psi_0 = 59 (\text{pH}_b - \text{pH}_s)$ mV, the ≈ 80 mV total change corresponds to a ≈ 1.3 increase

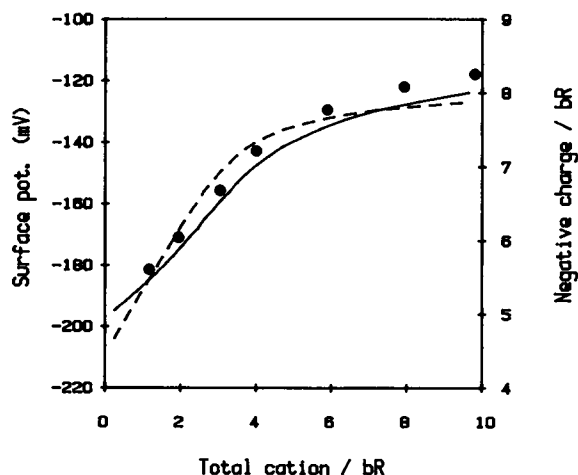


FIGURE 12 Changes in surface potential (—) and charge (---) during titration with divalent cations. No chemical binding, 10^{-5} M bR. Initial pH adjusted from 4 to 5 with NaOH. Composition as in Fig. 2. Experimental points from reference 31.

in surface pH. No chemical binding is assumed and the whole effect is due to charge screening and proton displacement by the added cations. The calculated potential change agrees well with the published experimental data (31). The number of net negative charges on the membrane surface increases as phosphate groups dissociate, finally reaches its limiting value, and the bR color turns purple (see Fig. 8), whereas the surface pH is still too low for carboxyl group dissociation. In cation titrations without readjustment of bulk pH, the calculated curves are very similar, only the initial value of the surface potential is now -220 mV and the number of charges is reduced by ≈ 2 (data not shown).

This calculation clearly demonstrates that the decrease in negative surface potential and increase in surface pH during cation titrations does not require cation binding and reduction of surface charge density. If chemical binding of cations and reduction in surface charge density are assumed, our calculations show, for binding constants 10 and 50 M^{-1} used as before, that the number of net negative charges gradually approaches 3 for MA_2 and 2 for MA^+ formation; the surface charge density decreases slightly if the pH is readjusted with NaOH and changes even less if the pH is not readjusted during the titration (data not shown). In our model, deionized blue membrane has a minimum of two negative charges per bR and this number does not decrease during cation addition in any of the cases discussed so far. Our model calculations, therefore, do not show the decrease in negative surface charge which one would expect if penetrating fields of bound cations were responsible for the color change.

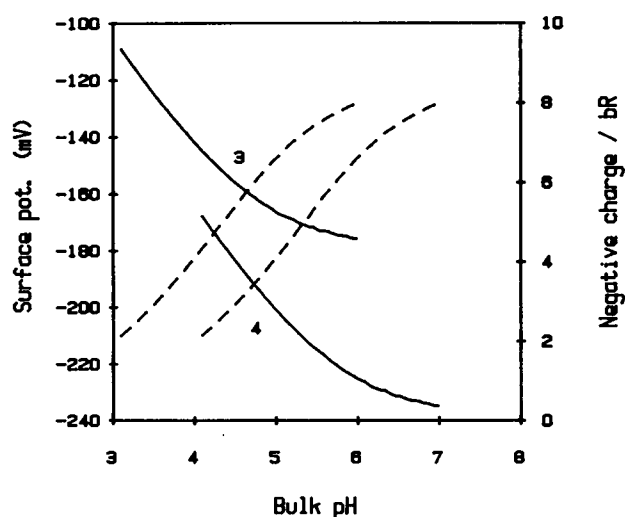


FIGURE 13 Changes in surface potential (—) and charge (---) during titration with base. Initial pH of blue membrane 3 and 4, bR 10^{-5} M , composition as in Fig. 2

In titration with NaOH (Fig. 13), the potential becomes more negative as bulk pH increases because, at low cation concentration, the bulk pH changes faster than the surface pH (see Figs. 2 and 3). Most of the potential change occurs before bR color starts changing (compare Figs. 10 and 13) which agrees with the experimental results (31). Because we assumed no chemical binding, the negative surface charge density gradually increases during titration. Note, that even in titration of blue membrane with initial pH 3, equivalent to 1 mM Na^+ , the bulk pH must rise above 7 before carboxyl ions appear (data not shown).

The dependence of surface potential and surface charge density on bulk pH in acid titration at constant salt concentration is shown in Fig. 14. At low salt concentration, there is a wide range of bulk pH where the blue membrane maintains two negative charges per bR. They are protonated only well below pH 2, and at that very low pH, the membrane becomes positively charged. However, it is probably incorrect to use the double layer theory in that high electrolyte concentration region, and instead, the charges should be considered discrete, and a more complicated theory is required (19). Because no chemical binding was assumed, the number of charges increases with increasing salt concentration. However, due to the screening effect of cations, the surface potential still decreases even when the surface carboxyls dissociate.

In addition to the reduced surface potential, the other significant difference between deionized and acid blue membranes is the much thinner double layer of acid blue

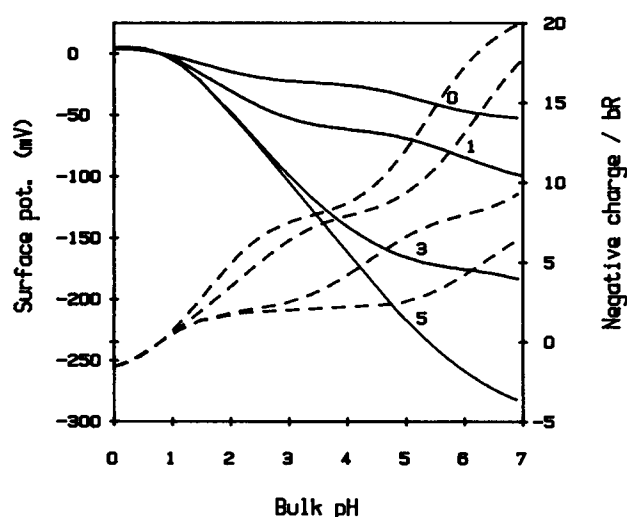


FIGURE 14 Changes in surface potential (—) and charge (---) during titration with acid at 10^0 , 10^{-1} , 10^{-3} , and 10^{-5} M monovalent cation concentrations. bR 10^{-5} M , composition as in Fig. 2

membranes. Due to the higher electrolyte concentration, the negative charges on the membrane are fully screened at much shorter distances and the electrostatic repulsive forces between membranes are less significant, which results in the well-known aggregation of the acid blue membranes. There is no need to assume structure differences between acid blue and deionized blue membranes to explain the aggregation, although some differences may exist because, at high electrolyte concentrations, the individual charges on the surface of acid blue membrane are also screened from one another.

We can conclude that to change the surface pH and color, cations need not be bound to surface charges in a chemical sense, and the membrane surface may carry even more negative charges in the purple than in the blue state. Depending on bulk pH and cation concentration, the surface potential may either increase or decrease when the surface pH increases and the color transition to purple occurs. Surface potential, charge density, and pH can only be used interchangeably if the concentrations in the bulk remain unchanged, which is often overlooked.

Scatchard plot of cation binding

Binding of cations to different sites of a protein is often described and analyzed by the Scatchard plot. While the free cation concentration in the bulk can be measured unambiguously, the determination of bound ions per protein depends on the method. In physical separation methods (filtration, centrifugation), the counterions in the double layer are removed, together with the membranes, and are considered bound. Techniques utilizing probe changes caused by environment or specific molecular interaction (e.g., ESR, luminescence) will count only those ions which are close to the surface groups. Even in the absence of chemical binding, some of the counterions are concentrated in a thin surface layer and may show different (bound) properties than ions in the bulk solution. In our calculations, we distinguish chemically bound from double layer bound cations, as previously discussed, and Scatchard plots can be constructed for either of them, as well as for the total bound cations.

Assuming no chemical binding, the Scatchard plot for the double layer-bound cations is shown in Fig. 15 for blue membrane titration with divalent cations. In this case, the released protons are not neutralized and the parameters correspond to the experimental conditions in reference 4. The agreement is satisfactory, considering the limitations of our model and the uncertainty in the experimental data for low cation concentrations.

Fig. 16 shows the calculated Scatchard plot for blue membrane titration with divalent cations at fixed bulk pH when no chemical binding is assumed and the bR concen-

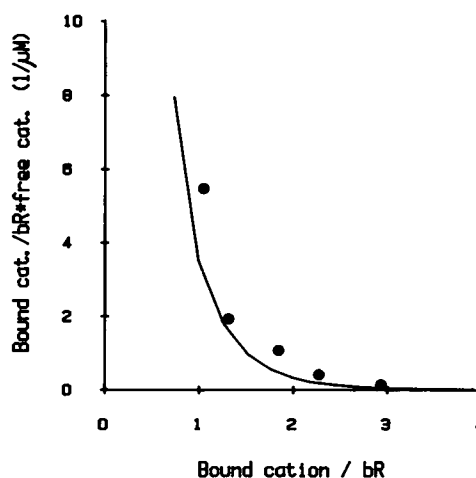


FIGURE 15 Calculated Scatchard plot for double layer-bound divalent cations. Initial blue membrane pH 5, bR $3 \cdot 10^{-5}$ M, no chemical binding, composition as in Fig. 2. Experimental points from reference 4.

tration is kept constant. Again, the calculated curve resembles the corresponding experimental one in reference 12; however, it is smooth and not composed of straight segments. The problems associated with the shape of the experimental Scatchard plot and its interpretation are beyond the scope of this paper and will be discussed elsewhere (see also reference 34). We only want to point out here that apparent binding constants similar to those calculated from the experimental curves can be derived from the calculated Scatchard plot, even though

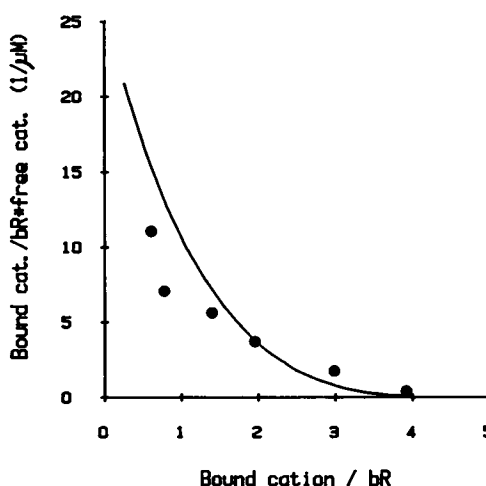


FIGURE 16 Calculated Scatchard plot for divalent cation binding in the double layer at pH 5. Blue membrane 10^{-5} M, initial pH adjusted from 4 to 5 with NaOH, no chemical binding, composition as in Fig. 2. Experimental points from reference 12.

no chemical binding, as in reference 12, was assumed in the calculations. Obviously, neither these apparent binding constants nor the corresponding binding sites have any physical meaning. The shape of the Scatchard plot does not change when chemical binding is introduced; the absolute values, however, differ and the "binding constants" increase (data not shown). These derived "binding constants" are six to eight orders of magnitude larger than the value used in the calculation ($K_b = 10$). The sum of chemically and double-layer-bound cations per bR is the same for either MA^+ or MA_2 and the chemically bound fraction is 70–80% for the MA^+ and ≈ 60 –70% for the MA_2 type of interaction. Using higher binding constants increases the chemically bound fraction.

DISCUSSION

We have shown here that, with reasonable assumptions about the membrane composition and surface charge density, the combination of dissociation and double layer theories allows one to calculate the surface pH and surface potential for a wide range of bulk pH and cation concentrations. From our earlier experimental work on pm with modified surface charge (14, 15), we had concluded that the purple-to-blue transition is governed by the surface pH only, and has an intrinsic pK between 1.5 and 2.0. Using this value, we have now derived theoretical titration curves which are in good agreement with published experimental curves. The generally postulated chemical binding of cations and direct effects of the changed electric field on the chromophore are not supported by our results. We will now discuss some additional work which has been used to argue for cation binding and direct field effects.

Our model is indeed supported by very recent experimental data on surface potential changes induced by Na^+ , Ca^{2+} , and La^{3+} additions to blue membrane at constant bulk pH (31), which the authors described as a unique relationship between bR color and surface potential changes regardless of the ion used. We interpret this experiment differently: bR color in native membrane is determined by surface pH. At constant bulk pH, $\Delta\psi_0 = 59 \times \Delta pH$, (millivolts) holds, and this equation is just another expression for the Boltzmann distribution, and, therefore, independent of any assumption made about the membrane. Because surface potential can be replaced by surface pH, and the reference state, the blue membrane, is common for all the cations studied, the surface pH corresponding to the same bR color is the same for all types of cations. As predicted by our model, the relation between surface potential and bR color is different in

other cases and it was indeed found in NaOH titration experiments (31).

The binding sites for cations are generally believed to be the carboxyl groups on the surface or in the protein, with the possible contribution of other groups forming coordination complexes (8, 9). Infrared spectroscopy showed protonation changes of carboxyls upon exposure of hydrated multilayers of blue membranes to NH_3 gas. However, the changes could only be related to water-exposed, surface carboxyl groups (35). These data do not support the concept of Schiff-base counterion protonation, but seem to agree with the interpretation of carboxyl involvement in the binding process. Our model calculations and earlier experiments indicate, however, that the color change occurs before carboxyl neutralization. Because most of the lipid phosphates and all the surface carboxyl groups in deionized blue membrane are protonated, addition of NH_3 will first titrate the lipid head groups, because they are stronger acids, and then the carboxyl groups. Similar results consistent with our conclusions have been obtained in another FTIR study, however, that study leaves open the possibility that an internal carboxyl group became protonated in the purple-to-blue transition (36). It is also very unlikely that the same carboxyl groups on the membrane surface can provide specific binding sites for all the mono-, di-, and trivalent cations which have been shown to be effective. The reported anomalous effects of Hg ions (9, 31) will be discussed elsewhere. No successful attempt has been reported so far on the localization of bound cation by structural methods. Published x-ray diffraction results (37) could not be confirmed in a reinvestigation (38).

That the purple-to-blue transition is not merely a double-layer phenomenon, but due to specific cation binding has been argued on the basis of temperature effects and the regeneration of blue and purple membrane from bleached and deionized membrane (8, 33). The formation of blue membrane at higher temperature is probably not related to surface pH changes predicted by dissociation or double-layer theories, but rather to a conformational change of the protein (39). We have shown that, at low ionic strength, the surface pH is well below the pK of carboxyl groups. Therefore, as pointed out earlier, any conformational change is likely to increase the number of positive charges because of the large number of Lys and Arg residues at or near the membrane surface, and so temperature and surface pH may lead to similar protein conformations. The same reasoning may be applied to the apparent decrease of binding sites in bleached membrane (8, 33), where CD directly shows a change of tertiary structure (40). We are aware of a publication which purports to show that the surface potentials in native and bleached membranes are

identical (41); however, the data are weak and the values reported for native membrane differ significantly from values reported by others (22, 42–44).

Luminescence changes associated with Eu^{3+} titration of blue membrane indicated a single binding constant but three binding sites were assumed, because a minimum of three components was required to fit the decay curves (29). The authors interpreted the sigmoidal titration curve as a cooperative field effect of the bound cations on bR conformation, on the chromophore and on the Schiff base pK. The binding sites were recently explicitly localized on the protein, because the lipid-depleted membrane showed essentially the same binding sites (45). We cannot fully accept these conclusions for the following reasons. The number of H_2O ligands to Eu^{3+} ions indicated that cations bind to the membrane surface. Because they replace a stoichiometric amount of H^+ , the net charge on the membrane surface cannot change appreciably and become much more positive upon cation binding. Local charge density changes due to di- and trivalent cations can not play a crucial role either, because monovalent cations are also effective in inducing bR color change. The binding sites cannot be identified unambiguously on the basis of luminescence data either, because it is known that Eu^{3+} binds to any negatively charged liposome, the luminescence of Eu^{3+} bound to either phosphatidylserine or phosphatidylglycerophosphate liposome has multiexponential decay characteristics, and the number of coordinated water molecules is very similar in both cases (46). Therefore, the added 3 Eu^{3+} /bR may bind to phospholipids in native membrane and to protein carboxyls in lipid-depleted membrane without showing any significant difference in the luminescence characteristics. Moreover, the lipid-depleted membrane still contains two or three lipid molecules per bR. Recent ^{31}P -NMR experiments indicated changes in the physical state of phosphate head groups upon addition of cations to deionized native membranes (32). It is also a rather interesting question why Eu^{3+} , presumably bound to the protein in the native and delipidated membranes, should determine the color in the native membrane, whereas it is unable to cause any change in the purple-to-blue transition of the delipidated membrane.²

The transition in the titrations applies to the state of the chromophore only; the surface properties, aggregation

state, etc., change continuously but are of secondary importance in this case. Most of the uncertainties in our results arise from the unknown distribution of acids and bases on the membrane surface, which we have overcome by choosing a reasonable composition to fit experimental data on the effect of lipid removal. We did not try, however, to find a best fit because our purpose was only to give a general picture of the phenomena. Nevertheless, the agreement with experimental data is unexpectedly good. At present, it seems to be more important to address the problem of differences in the surface properties of both sides of the membrane, which must be relevant because, in the pH range considered here, the asymmetry of charge distribution between the two sides reverses (47, 48). Attempts to determine experimentally from which side of the membrane the transition is driven have, so far, given conflicting results (49, 50).

In summary, we list our main conclusions, derived from this and also from our previous works (14, 15) on the purple-to-blue transition: (a) The color change of bR in pm is controlled entirely by surface proton concentration. (b) Cations have an indirect effect via raising the surface pH. (c) The effect of cations and pH on color can be quantitatively described by a surface model based on dissociation and double-layer theories. (d) The mechanism of color change involves conformational change of the protein, driven by protonation of its group(s), presumably resulting in charge rearrangement near the protonated Schiff base.

The surface phenomena discussed here, in relation to the purple-to-blue transition of bR, can be applied, in more general terms, to the purple membrane. The results we have presented are not directly relevant for the physiological environment of bR in halobacteria, because the salt concentration of KCl inside and NaCl outside the cell are near saturation. The results contribute, however, to our understanding of bR structure and function, especially of the chromophore-protein and lipid-protein interactions. Moreover, most investigations on which our present understanding are based have been carried out on isolated pm and in the 5–150 mM range of salt concentrations or on isolated bR in a neutral lipid environment. Little attention has been paid to differences in these parameters, when experimental results have been compared. Many apparent discrepancies, for instance in the kinetics and stoichiometry of the photoreaction cycle, may be resolved when we consider the differences in the effective pH at which the experiments were conducted.

In the preparation of this paper, we have benefitted from discussions with Dr. Yoshiaki Kimura and Dr. Roberto Bogomolni. We also thank Dr. S. McLaughlin and Dr. J. Cohen for their valuable comments on the manuscript.

²Here, we are considering only the fast, large absorption shift occurring in the blue-to-purple transition; several much smaller and slower absorption changes can be distinguished in kinetic experiments (4, 7, 50, 51) and also in the acid titration of pm (3). Since the fastest component(s) has not been time-resolved and the blue membrane is not a single species, i.e., at least a 13-*cis* and all-*trans* retinal conformer coexist, a satisfactory characterization of intermediates is presently impossible.

Received for publication 27 January 1989 and in final form 24 April 1989.

Note added in proof: After this manuscript had been submitted, we became aware of a paper by Steward, L. C., M. Kates, and I. C. P. Smith (1988. *Chem. Phys. Lipids*. 48:177–188). They titrated phosphatidylglycerophosphate in an aqueous suspension and found a $pK \approx 2.4$ in the presence of 0.1 M KCl. Because of the high charge density on the surface of lipid micelles or vesicles employed in the study, the intrinsic pK and the surface pH are probably 1 U lower and do not contradict our results.

REFERENCES

- Oesterhelt, D., and W. Stoeckenius. 1971. Rhodopsin-like protein from the purple membrane of *Halobacterium halobium*. *Nat. New Biol.* 233:149–152.
- Moore, T. A., M. E. Edgerton, G. Parr, C. Greenwood, and R. N. Perham. 1978. Studies of an acid-induced species of purple membrane from *Halobacterium halobium*. *Biochem. J.* 171:469–476.
- Mowery, P. C., R. H. Lozier, Q. Chae, Y.-W. Tseng, M. Taylor, and W. Stoeckenius. 1979. Effect of acid pH on the absorption spectra and photoreactions of bacteriorhodopsin. *Biochemistry*. 18:4100–4107.
- Kimura, Y., A. Ikegami, and W. Stoeckenius. 1984. Salt and pH-dependent changes of the purple membrane absorption spectrum. Evidence for changes in conformation of the protein. *Photochem. Photobiol.* 40:641–646.
- Smith, S. O., and R. A. Mathies. 1985. Resonance Raman spectra of the acidified and deionized forms of bacteriorhodopsin. *Biophys. J.* 47:251–254.
- Chang, C.-H., J. G. Chen, R. Govindjee, and T. Ebrey. 1985. Cation binding by bacteriorhodopsin. *Proc. Natl. Acad. Sci. USA*. 82:396–400.
- Fischer, U., and D. Oesterhelt. 1979. Chromophore equilibria in bacteriorhodopsin. *Biophys. J.* 28:211–230.
- Chang, C.-H., R. Jonas, S. Melchior, R. Govindjee, and T. G. Ebrey. 1986. Mechanism and role of divalent cation binding of bacteriorhodopsin. *Biophys. J.* 49:731–739.
- Ariki, M., and J. K. Lanyi. 1986. Characterization of metal ion binding sites in bacteriorhodopsin. *J. Biol. Chem.* 261:8167–8174.
- Chronister, E. L., T. C. Corcoran, L. Song, and M. A. El-Sayed. 1986. On the molecular mechanism of the Schiff base deprotonation during the bacteriorhodopsin photocycle. *Proc. Natl. Acad. Sci. USA*. 83:8580–8584.
- Chronister, E. L., and M. A. El-Sayed. 1987. Time-resolved resonance Raman spectra of the photocycle intermediates of acid and deionized bacteriorhodopsin. *Photochem. Photobiol.* 45:507–513.
- Dunach, M., M. Seigneuret, J.-L. Rigaud, and E. Padros. 1987. Characterization of the cation binding sites of the purple membrane. Electron spin resonance and flash photolysis studies. *Biochemistry*. 26:1179–1186.
- Dunach, M., M. Seigneuret, J.-L. Rigaud, and E. Padros. 1986. The relationship between the chromophore moiety and the cation binding sites in bacteriorhodopsin. *Biosci. Rep.* 6:961–966.
- Szundi, I., and W. Stoeckenius. 1987. Effect of lipid surface charges on the purple-to-blue transition of bacteriorhodopsin. *Proc. Natl. Acad. Sci. USA*. 84:3681–3684.
- Szundi, I., and W. Stoeckenius. 1988. Purple-to-blue transition of bacteriorhodopsin in a neutral lipid environment. *Biophys. J.* 54:227–232.
- Blaurock, A. E., and W. Stoeckenius. 1971. Structure of the purple membrane. *Nat. New Biol.* 233:152–155.
- Kates, M., S. C. Kushwaha, and G. D. Sprott. 1982. Lipids of purple membrane from extreme halophiles and of methanogenic bacteria. *Methods Enzymol.* 88:98–111.
- McLaughlin, S. 1977. Electrostatic potentials at membrane-solution interfaces. *Curr. Top. Membr. Transp.* 9:71–144.
- Winiski, A. P., A. C. McLaughlin, R. V. McDaniel, M. Eisenberg, and S. McLaughlin. 1986. An experimental test of the discreteness-of-charge effect in positive and negative lipid bilayers. *Biochemistry*. 25:8206–8214.
- Amory, D. E., and J. E. Dufey. 1985. Model for the electrolytic environment and electrostatic properties of biomembranes. *J. Bioenerg. Biomembr.* 17:151–174.
- Henderson, R., J. S. Jubb, and S. Whytock. 1978. Specific labelling of the protein and lipid on the extracellular surface of purple membrane. *J. Mol. Biol.* 123:259–274.
- Renthal, R., and C.-H. Cha. 1984. Charge asymmetry of the purple membrane measured by uranyl quenching of dansyl fluorescence. *Biophys. J.* 45:1001–1006.
- Jost, P. C., D. A. McMillen, W. D. Morgan, and W. Stoeckenius. 1978. Lipid-protein interactions in the purple membrane. In *Light Transducing Membranes: Structure, Function, and Evolution*. Academic Press, Inc., New York. 141–155.
- Glaeser, R. M., J. S. Jubb, and R. Henderson. 1985. Structural comparison of native and deoxycholate-treated purple membrane. *Biophys. J.* 48:775–780.
- Engelman, D. M., A. Goldman, and T. A. Steitz. 1982. The identification of helical segments in the polypeptide chain of bacteriorhodopsin. *Methods Enzymol.* 88:81–88.
- Neugebauer, D. C. 1975. An attempt to develop a reliable method of orienting the purple membranes of *Halobacterium halobium* for x-ray diffraction studies. Ph.D. thesis. Julius-Maximilians-Universitaet-Wuerzburg, FRG.
- Lau, A., A. McLaughlin, and S. McLaughlin. 1981. The adsorption of divalent cations to phosphatidylglycerol bilayer membranes. *Biochim. Biophys. Acta*. 645:279–292.
- Bakker-Grunwald, T., and B. Hess. 1981. Interactions of bacteriorhodopsin containing membrane systems with polyelectrolytes. *J. Memb. Biol.* 60:45–49.
- Corcoran, T. C., K. Z. Ismail, and M. A. El-Sayed. 1987. Evidence for the involvement of more than one metal cation in the Schiff base deprotonation process during the photocycle of bacteriorhodopsin. *Proc. Natl. Acad. Sci. USA*. 84:4094–4098.
- Dunach, M., E. Padros, M. Seigneuret, and J.-L. Rigaud. 1988. On the molecular mechanism of the blue to purple transition of bacteriorhodopsin. UV-difference spectroscopy and electron spin resonance studies. *J. Biol. Chem.* 263:7555–7559.
- Dunach, M., M. Seigneuret, J.-L. Rigaud, and E. Padros. 1988. Influence of cations on the blue to purple transition of bacteriorhodopsin: comparison of Ca^{2+} and Hg^{2+} binding, and their effect on the surface potential. *J. Biol. Chem.* 263:17378–17384.
- Roux, M., M. Seigneuret, and J.-L. Rigaud. 1988. ^{31}P NMR study

- of the interaction of cations with purple membrane and of the purple-blue transition. *Biochemistry*. 27:7009–7015.
33. Chang, C.-H., R. Jonas, R. Govindjee, and T. G. Ebrey. 1988. Regeneration of blue and purple membranes from deionized bleached membranes of *Halobacterium halobium*. *Photochem. Photobiol.* 47:261–265.
 34. McLaughlin, S., and H. Harary. 1976. The hydrophobic adsorption of charged molecules to bilayer membranes: a test of the applicability of the Stern equation. *Biochemistry*. 15:1941–1948.
 35. Gerwert, K., U. M. Ganter, F. Seibert, and B. Hess. 1987. Only water-exposed carboxyl groups are protonated during the transition to the cation-free blue bacteriorhodopsin. *FEBS (Fed. Eur. Biochem. Soc.) Lett.* 213:39–44.
 36. Marrero, H., and K. J. Rothschild. 1987. Conformational changes in bacteriorhodopsin studied by infrared attenuated total reflection. *Biophys. J.* 52:629–635.
 37. Katre, N. V., Y. Kimura, and R. M. Stroud. 1986. Cation binding sites on the projected structure of bacteriorhodopsin. *Biophys. J.* 50:277–284.
 38. Dudda, C. 1987. Roentgenstrukturuntersuchungen zur lokalisation der kationenbindungsstellen in der purpurnmembran von *Halobacterium halobium*. Ph.D. thesis. Freie Universitaet Berlin.
 39. Scherrer, P., M. K. Mathew, W. Sperling, and W. Stoeckenius. 1989. Retinal isomer ration in dark-adapted purple membrane and bacteriorhodopsin monomers. *Biochemistry*. 28:829–834.
 40. Becher, B., and J. Y. Cassim. 1977. Effects of bleaching and regeneration on the purple membrane structure of *Halobacterium halobium*. *Biophys. J.* 19:285–297.
 41. Ehrenberg, B., and Z. Meiri. 1983. The bleaching of purple membranes does not change their surface potential. *FEBS (Fed. Eur. Biochem. Soc.) Lett.* 164:63–66.
 42. Packer, L., B. Arrio, G. Johannin, and P. Volfin. 1984. Surface charge of purple membranes by laser doppler velocimetry. *Biochem. Biophys. Res. Commun.* 122:252–258.
 43. Carmeli, C., A. T. Quintanilha, and L. Packer. 1980. Surface charge changes in purple membrane and the photoreaction cycle of bacteriorhodopsin. *Proc. Natl. Acad. Sci. USA*. 77:4704–4711.
 44. Cafiso, D. S., W. L. Hubbell, and A. Quintanilha. 1982. Spin-label probes of light-induced electrical potentials in rhodopsin and bacteriorhodopsin. *Methods Enzymol.* 88:682–696.
 45. Jang, D.-J., and M. A. El-Sayed. 1988. Deprotonation of lipid-depleted bacteriorhodopsin. *Proc. Natl. Acad. Sci. USA*. 85:5918–5922.
 46. Herrmann, T. R., A. R. Jayaweera, and A. E. Shamo. 1986. Interaction of Europium (III) with phospholipid vesicles as monitored by laser-excited Europium (III) luminescence. *Biochemistry*. 25:5834–5838.
 47. Fisher, K. A., K. Yanagimoto, and W. Stoeckenius. 1978. Oriented adsorption of purple membrane to cationic surfaces. *J. Cell Biol.* 77:611–621.
 48. Zingsheim, H. P., D. C. Neugebauer, and R. Henderson. 1978. Properties of the two sides of the purple membrane correlated. *J. Mol. Biol.* 123:275–278.
 49. Lind, C., B. Hojeberg, and H. G. Khorana. 1981. Reconstitution of delipidated bacteriorhodopsin with endogenous polar lipids. *J. Biol. Chem.* 256:8298–8305.
 50. Druckmann, S., M. Ottolenghi, and R. Korenstein. 1985. Time-resolved absorbance changes induced by fast acidification of bacteriorhodopsin in vesicle systems. *Biophys. J.* 47:115–118.
 51. Zubov, B., K. Tsuji, and B. Hess. 1986. Transient kinetics of the conversion of blue to purple bacteriorhodopsin upon magnesium binding. *FEBS (Fed. Eur. Biochem. Soc.) Lett.* 200:226–230.